Translating biased signaling in the ghrelin receptor system into differential in vivo functions

Franziska Mende[a,b,1], Cecilie Hundahl[a,b,1], Bianca Plouffe[c,d,1], Louise Julie Skov[a,b], Bjørn Sivertsen[a,b], Andreas Nygaard Madsen[a,b], Michael Lückmann[b], Thi Ai Diep[a,b], Stefan Offermanns[e,f,g], Thomas Michael Frimurer[b], Michel Bouvier[c,d,2], and Birgitte Holst[a,b,2]

[a]Laboratory for Molecular Pharmacology, Department of Biomedical Sciences, University of Copenhagen, DK-2200 Copenhagen, Denmark; [b]Section for Metabolic Receptology, Novo Nordisk Foundation Center for Basic Metabolic Research, University of Copenhagen, DK-2200 Copenhagen, Denmark; [c]Department of Biochemistry and Molecular Medicine, Université de Montréal, Montréal, QC H3C IJ4, Canada; [d]Institute for Research in Immunology and Cancer, Université de Montréal, Montréal, QC H3C IJ4, Canada; [e]Max Planck Institute for Heart and Lung Research, Johan Wolfgang Goethe University Frankfurt, 60323 Frankfurt, Germany; [f]Department of Pharmacology, Johan Wolfgang Goethe University Frankfurt, 60323 Frankfurt, Germany; and [g]Centre for Molecular Medicine, Medical Faculty, Johan Wolfgang Goethe University Frankfurt, 60323 Frankfurt, Germany

Edited by Robert J. Lefkowitz, Howard Hughes Medical Institute and Duke University Medical Center, Durham, NC, and approved September 18, 2018 (received for review March 7, 2018)

Biased signaling has been suggested as a means of selectively modulating a limited fraction of the signaling pathways for G-protein–coupled receptor family members. Hence, biased ligands may allow modulation of only the desired physiological functions and not elicit undesired effects associated with pharmacological treatments. The ghrelin receptor is a highly sought antiobesity target, since the gut hormone ghrelin in humans has been shown to increase both food intake and fat accumulation. However, it also modulates mood, behavior, growth hormone secretion, and gastric motility. Thus, blocking all pathways of this receptor may give rise to potential side effects. In the present study, we describe a highly promiscuous signaling capacity for the ghrelin receptor. We tested selected ligands for their ability to regulate the various pathways engaged by the receptor. Among those, a biased ligand, YIL781, was found to activate the $G\alpha_{q/11}$ and $G\alpha_{12}$ pathways selectively without affecting the engagement of β-arrestin or other G proteins. YIL781 was further characterized for its in vivo physiological functions. In combination with the use of mice in which $G\alpha_{q/11}$ was selectively deleted in the appetite-regulating AgRP neurons, this biased ligand allowed us to demonstrate that selective blockade of $G\alpha_{q/11}$, without antagonism at β-arrestin or other G-protein coupling is sufficient to decrease food intake.

biased signaling | ghrelin receptor | appetite regulation | food intake | gastric emptying

Ghrelin is a gut hormone that stimulates food intake and adiposity. It has been shown to act on a G-protein–coupled receptor (GPCR), the ghrelin receptor (GhrR), in the hypothalamic arcuate nucleus, where it increases the activity of the neuropeptide Y (NPY)/Agouti-related peptide (AgRP)-expressing neurons and simultaneously inhibits proopiomelanocortin (POMC)-expressing neurons through GABA-mediated transmission (1). Thus, GhrR is an attractive target in the development of antiobesity treatment. However, GhrR signaling is also involved in several other functions, including gastrointestinal motility, mood and behavioral regulation, and growth hormone secretion (2). These diverse functions contribute significantly to the major challenge in developing small-molecule drugs that selectively modulate appetite, food intake, and body weight via the receptor. Antagonists could also affect other physiological functions regulated by the GhrR, causing potential side effects.

However, the concept of ligand bias offers an approach to tackle this issue. The GhrR is a promiscuous seven-transmembrane (7TM) receptor signaling through numerous different pathways including both G-protein–dependent and –independent (3) mechanisms. Individual pathways, if selectively stimulated, may lead to isolated physiological outcomes (4). Thus, it is critical to identify the physiological functions associated with each of these GhrR-mediated pathways in the hope of developing drugs that selectively target appetite regulation.

Activation of the GhrR induces calcium release, generally assumed to be part of the $G\alpha_q$ signaling pathway, via phospholipase C activation and the resulting increase inositol triphosphate (IP_3) production (5). GhrR-promoted $G\alpha_{i/o}$ activation has been demonstrated in GTPγS assays (6), in bioluminescence resonance energy transfer (BRET)-based assays, and in isolated lipid discs (7). $G\alpha_{12/13}$ coupling has been suggested using specific pathway inhibitors (2). Finally, GhrR activation leads to the recruitment of β-arrestins (7, 8). The endogenous full agonist, ghrelin, activates the entire signaling repertoire, leading to various biological functions. In contrast, functionally selective agonists or antagonists, i.e., biased ligands (9–11), would activate or block only a subset of the signaling repertoire, thus opening the possibility of targeting only the physiologically beneficial pathways and not those associated with unwanted detrimental effects. Such ligands that differentiate between G-protein–dependent and –independent pathways have been described for other receptors (4). For instance, β-arrestin–selective agonists have been reported for the β1-adrenergic (12), the parathyroid hormone

Significance

Obesity is a major health threat of the twenty-first century, impacting individual patients and healthcare expenditure. Due to safety concerns, few antiobesity treatments with only moderate effect remain on the market. The ghrelin receptor is an attractive target for the development of novel antiobesity drugs, since ghrelin increases both fat accumulation and food intake. However, ghrelin also modulates a variety of additional physiological functions. Thus, drugs targeting the ghrelin receptor may induce unacceptable side effects and have limited clinical use. We demonstrate that biased ligands, which selectively activate only a subset of the molecular signaling pathways, may be powerful tools to obtain drugs that efficaciously reduce body weight without inducing adverse effects by selectively modulating appetite and energy expenditure.

Author contributions: M.B. and B.H. designed research; F.M., C.H., B.P., L.J.S., B.S., A.N.M., M.L., and T.A.D. performed research; S.O. contributed new reagents/analytic tools; F.M., C.H., B.P., L.J.S., B.S., T.M.F., and B.H. analyzed data; and F.M., C.H., B.P., M.B., and B.H. wrote the paper.

The authors declare no conflict of interest.

This article is a PNAS Direct Submission.

[1]F.M., C.H., and B.P. contributed equally to this work.

[2]To whom correspondence may be addressed. Email: michel.bouvier@umontreal.ca or holst@sund.ku.dk.

This article contains supporting information online at www.pnas.org/lookup/suppl/doi:10.1073/pnas.1804003115/-/DCSupplemental.

Published online October 9, 2018.

(PTH) (13, 14), the dopamine D2 (15, 16), and the angiotensin type 1 (AT1) receptors (17). Examples of clinically promising biased agonists are the μ-opioid receptor ligands TRV130 and PZV21, biased for $G\alpha_i$ activation over β-arrestin recruitment. These ligands display an efficacious analgesic effect with limited side effects (such as respiratory depression and constipation) in animal models (18–20). In a recent phase IIb clinical trial, TRV130 was found to be as efficacious an analgesic as morphine, and its side effects related to nausea, vomiting, and respiratory function were reduced compared with morphine. Although more studies are needed to confirm the possible advantages of biased ligands and whether the concept could be applicable to other therapeutically relevant GPCRs, these studies open exciting avenues for the discovery of a new generation of safer drugs.

In the present study, we selected two small-molecule GhrR ligands, the Bayer compound YIL781 and the Abbott compound Abb13d, which were originally developed as GhrR antagonists, and analyzed their properties in several signaling pathways to assess whether they display biased activities. We report that, while both compounds are weak inverse agonists for β-arrestin recruitment and both inhibit the gastric emptying associated with nausea, they differentially regulate the $G\alpha_{q/11}$ pathway. Abb13d is an inverse agonist for $G\alpha_{q/11}$-associated signals, while YIL781 is a partial agonist for this pathway. The two compounds also had different in vivo effects on food intake, suggesting that the appetite-modulatory effect resulted from an action on the $G\alpha_{q/11}$ pathway. This role of $G\alpha_{q/11}$ in appetite regulation was confirmed in a genetic murine model selectively lacking $G\alpha_q$ and $G\alpha_{11}$ in the arcuate nucleus of the hypothalamus.

Results

Binding Properties. The binding properties of ghrelin and five small-molecule ligands (21, 22) developed to antagonize GhrR were assessed in HEK293 cells transiently transfected with wild-type human GhrR (*SI Appendix*, Table S1). All the compounds bound to the GhrR with high affinity, as estimated by binding-competition assays using [^{3}H]-MK677 as the radioligand. The affinities estimated based on the K_i values varied between 0.09 nM and 10 nM (Fig. 1*A* and *SI Appendix*, Table S1).

Functional Evaluation.

Second messenger for the $G\alpha_{q/11}$ pathway. GhrR is described as a primarily $G\alpha_{q/11}$-coupled receptor. Thus, pharmaceutical drug-discovery programs have used Ca^{2+} mobilization measurements to identify GhrR antagonists, since this assay allows high-throughput screening (5, 23). We evaluated the antagonistic properties of the five compounds at ∼80% of the maximal efficacy of ghrelin. The apparent IC_{50} of the antagonists in the calcium (Fig. 1*B*) and inositol phosphate (IP) (Fig. 1*D*) assays varied from 1 nM to more than 1,000 nM (*SI Appendix*, Table S1). Although the potencies and binding affinities correlated relatively well for most compounds, a significant difference was found for Abb13d, which showed a 100-fold apparent lower potency than its binding affinity determined in competition binding. This discrepancy most likely results from probe dependency (24), since the binding affinity was determined using [^{3}H]-MK677 as the tracer, whereas the functional antagonism was assessed using ghrelin as the agonist. Notably, YIL781 did not display partial agonism when tested for antagonism in the calcium assay (Fig. 1*B*), most likely due to the transient nature of the calcium response, i.e., the YIL781-induced calcium peak had returned to basal level at the time of ghrelin administration.

When the compounds were tested for their intrinsic ability to stimulate calcium release, YIL781, Glaxo755053, and JMV3002 were found to be partial agonists with efficacies of 20%, 20%, and 13% of ghrelin-induced stimulation, respectively, and with potencies similar to their binding affinities (Fig. 1*C* and *SI Appendix*, Table S1). JMV3002 differed slightly from the other

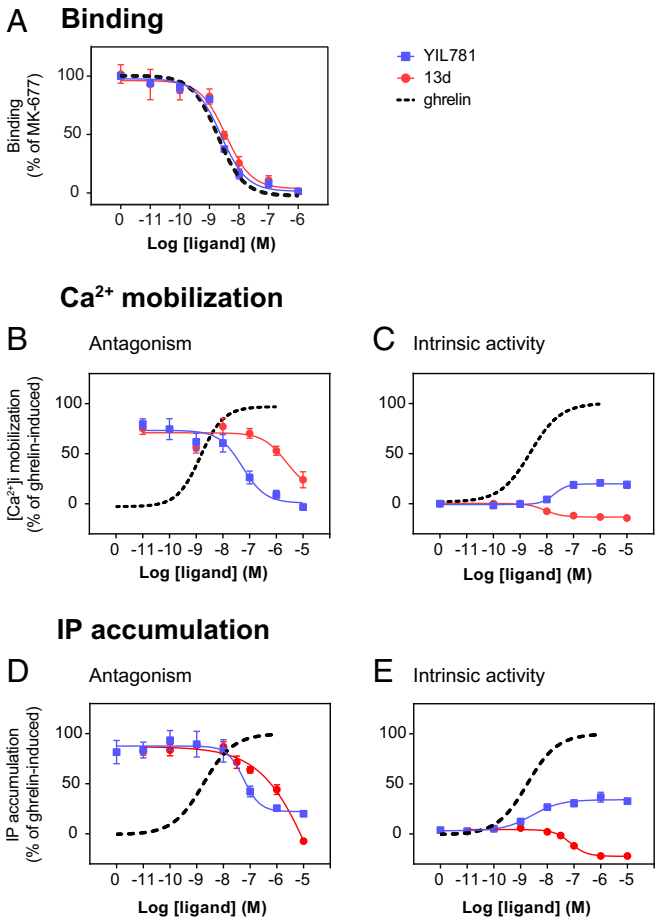

Fig. 1. Binding properties and second-messenger responses induced by ghrelin, YIL781, and Abb13d. (*A*) Competition binding of ghrelin (black dashed line), YIL781 (blue line) and 13d (red line) using 3H-labeled MK-677 as a radioligand. (*B*) YIL781 and Abb13d antagonize Ca^{2+} mobilization induced by 10 nM ghrelin. (*C*) When measuring the intrinsic activity of the compounds, YIL781 turned out to be a partial agonist, and Abb13d was found to be an inverse agonist for inducing Ca^{2+} release. (*D*) YIL781 and Abb13d also antagonize the IP response induced by 10 nM ghrelin. (*E*) YIL781 is a partial agonist and Abb13d is an inverse agonist for stimulation of IP signaling. Data points are the mean ± SEM of three to five independent experiments performed in triplicate.

compounds, as its partial agonist potency in the calcium-release assay was almost 100-fold lower than its potency in IP accumulation, the latter being more consistent with its binding affinity. Only two compounds, Abb13d and Abb14c, were found to be weak inverse agonists. The inverse agonist potency of Abb13d was similar to its binding affinity, but the inverse efficacy of Abb14c was too weak to calculate an EC_{50} reliably. Such low apparent efficacy is most likely due to the low and inconsistent level of constitutive activity revealed by the calcium-release assays (25). This was confirmed by the IP assay used as an additional readout for the $G\alpha_{q/11}$-promoted phospholipase C (PLC) activity. Indeed, the inverse efficacy of both Abb13d and Abb14c was readily observed, with inverse efficacies of −23% and −26% and potencies of 76 nM and 10 nM, respectively (Fig. 1*E* and *SI Appendix*, Table S1). As in the calcium assay, YIL781, Glaxo755053, and JMV3002 were found to be partial agonists in the IP assay, with efficacies ranging from 29% to 41% of ghrelin-induced stimulation (Fig. 1*E* and *SI Appendix*, Table S1). In the interest of simplicity, we show only two representative ligands—one partial agonist (YIL781), and one inverse agonist (Abb13d)—in Fig. 1.

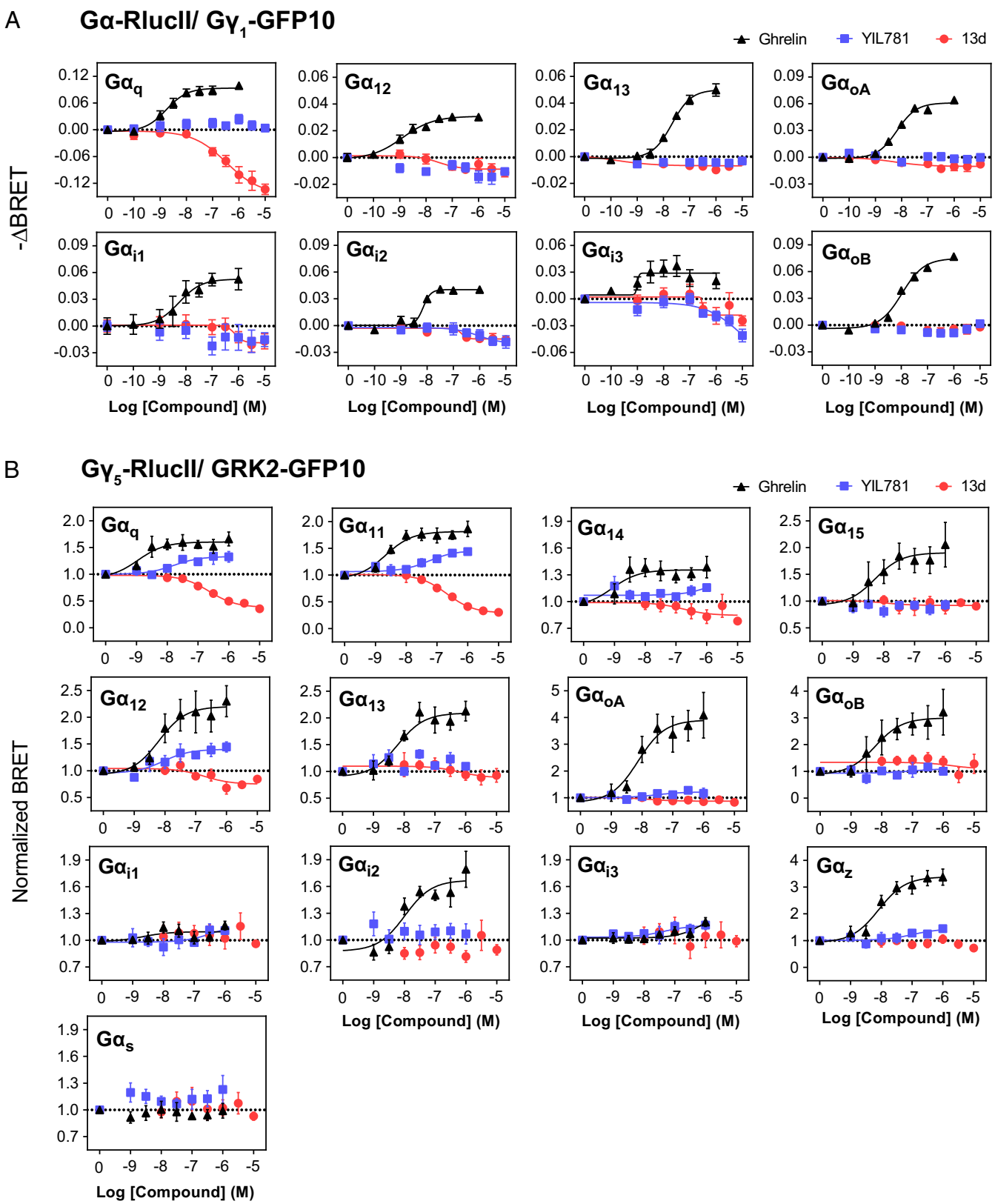

Fig. 2. Differential panel of G-protein activation by ghrelin, YIL781, and Abb13d, shown by two distinct BRET biosensors. Dose-dependent activation by ghrelin (black), YIL781 (blue), and Abb13d (red) of $G\alpha_{q/11}$, $G\alpha_{i/o}$, $G\alpha_{12/13}$, and $G\alpha_s$ proteins shown by Gα-RlucII/GFP10-$G\gamma_1$ BRET biosensors (*A*) and RlucII-$G\gamma_5$/GRK2-GFP10 BRET biosensors (*B*). Data points are the mean ± SEM of three to five independent experiments performed in triplicate. Ghrelin is a full agonist activating isoforms of all Gα protein families, whereas YIL781 and Abb13d signal only via proteins of the $G\alpha_{q/11}$ and $G\alpha_{12/13}$ families.

To confirm that the Ca^{2+} mobilization resulted from $G\alpha_{q/11}$ activation, we tested ghrelin-induced Ca^{2+} mobilization in the presence of G_i (pertussis toxin, PTX), Gβγ (gallein) (26), or $G\alpha_q$/$G\alpha_{11}$/$G\alpha_{14}$ (UBO-QIC) (27) inhibitors. Only the $G\alpha_{q/11/14}$ inhibitor abrogated Ca^{2+} mobilization (*SI Appendix*, Fig. S1*A*), confirming the prominent role of this pathway in the calcium response. This was further confirmed by the observation that no ghrelin-induced calcium response could be observed in cells in which $G\alpha_{q/11}$ was genetically deleted unless $G\alpha_q$, $G\alpha_{11}$, or $G\alpha_{14}$ was reintroduced in the cells (*SI Appendix*, Fig. S1*B*).

In summary, our results demonstrate that some compounds developed as antagonists behave as partial agonists in second-messenger assays downstream of $G\alpha_{q/11}$, whereas others have negative intrinsic activity and are inverse agonists. Based on these observations, we selected one of the partial agonists (YIL781) and one of the inverse agonists (Abb13d) for further analysis.

Monitoring G-protein activation. To confirm the difference in the intrinsic efficacy between YIL781 and Abb13d, we assessed the direct activation of G proteins using BRET-based biosensors, an approach that prevents interference from amplification or crosstalk between downstream effector systems. First, we used an assay that monitors the separation between Gα and Gβγ subunits upon G-protein activation by measuring BRET between Gα subunits fused to the energy donor, RlucII, and Gγ1 fused to the energy acceptor, GFP10, in the presence of unlabeled Gβ1. The activation results in a decrease in BRET signal, and the amplitude of this signal is used as an index of the G-protein activation (28). As shown in Fig. 2, in addition to activating $G\alpha_q$, ghrelin was able to activate $G\alpha_{12}$ and $G\alpha_{13}$ as well as members of the $G\alpha_{i/o}$ family. As suggested by the second-messenger assays, YIL781 and Abb13d had distinct intrinsic efficacies. Whereas Abb13d was a robust inverse agonist for $G\alpha_q$ with a potency of 335 nM, YIL781 did not show any detectable intrinsic activity in this assay. No intrinsic activity of either compound could be detected for any of the other G proteins that were activated by ghrelin; thus both YIL781 and Abb13d behaved as neutral antagonists for these pathways under the conditions studied.

To test whether the partial agonism detected for YIL781 using the second-messenger assays could be revealed at the G-protein level, we used a second BRET-based assay that is more sensitive in detecting the activation of $G\alpha_{q/11}$ family members. This biosensor monitors the competition between Gα and GPCR kinase-2 (GRK2) for their interaction with Gβγ by measuring BRET between GRK2-GFP10 and RlucII-Gγ5 upon overexpression of each individual unlabeled Gα subunit. The separation of Gβγ from the Gα subunit upon receptor activation results in an increase in BRET between GRK2-GFP10 and RlucII-Gγ5. Because GRK2 harbors an RGS domain for $G\alpha_q$, it is particularly sensitive in detecting G_q activation. As can be seen in Fig. 2, the ability of ghrelin to activate $G\alpha_{q/11}$, $G\alpha_{i/o}$, and $G\alpha_{12/13}$ family members could be confirmed with this biosensor, although the activation signals observed for $G\alpha_{i1}$ and $G\alpha_{i3}$ were smaller and could not be fitted to concentration–response curves. As was observed with the Gα/Gβγ separation assay, both $G\alpha_{12}$ and $G\alpha_{13}$ could be activated by ghrelin. As expected, no activation of $G\alpha_s$ was detected.

Upon testing Abb13d and YIL781 with the GRK2-based sensor, the inverse agonism of Abb13d was confirmed not only for $G\alpha_q$ but also for another member of the $G\alpha_{q/11}$ family, $G\alpha_{11}$, with IC_{50} values of 229 nM and 209 nM, respectively (Fig. 2 and *SI Appendix*, Table S2). In this assay, the partial agonism of YIL781 was revealed with EC_{50}s of 16 nM and 53 nM, activating both $G\alpha_q$ and $G\alpha_{11}$ with 45% and 43% of ghrelin efficacy, respectively, confirming the results obtained from the second-messenger assays. This assay also confirmed the lack of intrinsic activity of the two compounds toward the $G\alpha_{i/o}$ family members. However, a significant partial agonism toward $G\alpha_{12}$, but not $G\alpha_{13}$, could be detected for YIL781, indicating that it could also be a weak partial agonist for this pathway (Fig. 2 and *SI Appendix*, Table S2). Neither Abb13d nor YIL781 had significant intrinsic activity toward $G\alpha_{14}$ or $G\alpha_{15}$.

Monitoring β-arrestin recruitment. BRET between β-arrestin1/2-RlucII and rGFP-CAAX was used to measure the recruitment of β-arrestins to the cell membrane upon receptor stimulation. β-Arrestins are involved in the attenuation of the G-protein signaling and internalization of the receptor but also initiate G-protein–independent signaling cascades, possibly leading to distinct physiological effects. Ghrelin induced recruitment of both β-arrestin 1 and 2, with apparent potencies of 12 nM and 14 nM, respectively (Fig. 3). Both YIL781 and Abb13d antagonized the ghrelin-induced recruitment of β-arrestin 1, with potencies of 314 nM and 2.3 μM, respectively (Fig. 3*A*), and the ghrelin-induced recruitment of β-arrestin 2, with potencies of 414 nM and 2.5 μM, respectively (Fig. 3*C*). Analysis of the intrinsic activity of the two compounds showed very little intrinsic efficacy, YIL781 and Abb13d having a tendency toward inverse agonism (Fig. 3 *B* and *D*).

Mapping of Receptor Interaction Epitopes. To determine the molecular differences responsible for the functional activity observed for the partial agonist YIL781 compared with the inverse agonists from Abbott, we conducted a targeted mutational study. We used IP-accumulation assays as a functional readout, since the differences in intrinsic activity were most pronounced in this functional assay. As the inverse agonist, we selected the most potent and high-affinity ligand, Abb14c.

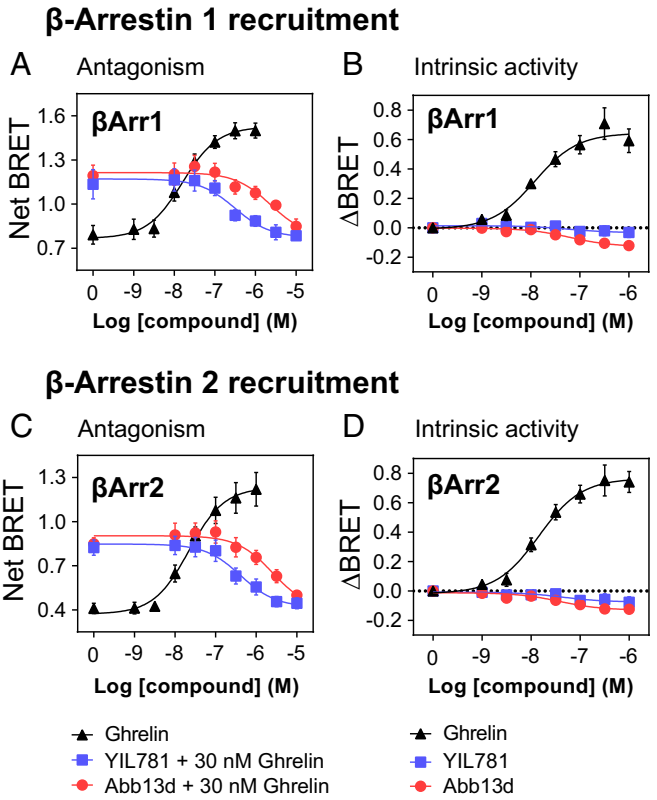

Fig. 3. GhrR-mediated signaling through β-arrestins. (*A* and *C*) YIL781 and Abb13d antagonize β-arrestin 1 recruitment (*A*) and β-arrestin 2 recruitment (*C*) induced by 30 nM ghrelin. (*B* and *D*) YIL781 and Abb13d are weak inverse agonists in terms of their intrinsic activity to recruit β-arrestin 1 (*B*) and β-arrestin 2 (*D*). Data points are the mean ± SEM of five to eight independent experiments performed in triplicate.

Residues selected for mutagenesis were based on previous studies characterizing receptor-recognition epitopes (29, 30). The only other GhrR antagonists that have previously been studied for their receptor-interaction patterns are peptide inverse agonists (31). Small-molecule antagonists and inverse agonists have never been mapped.

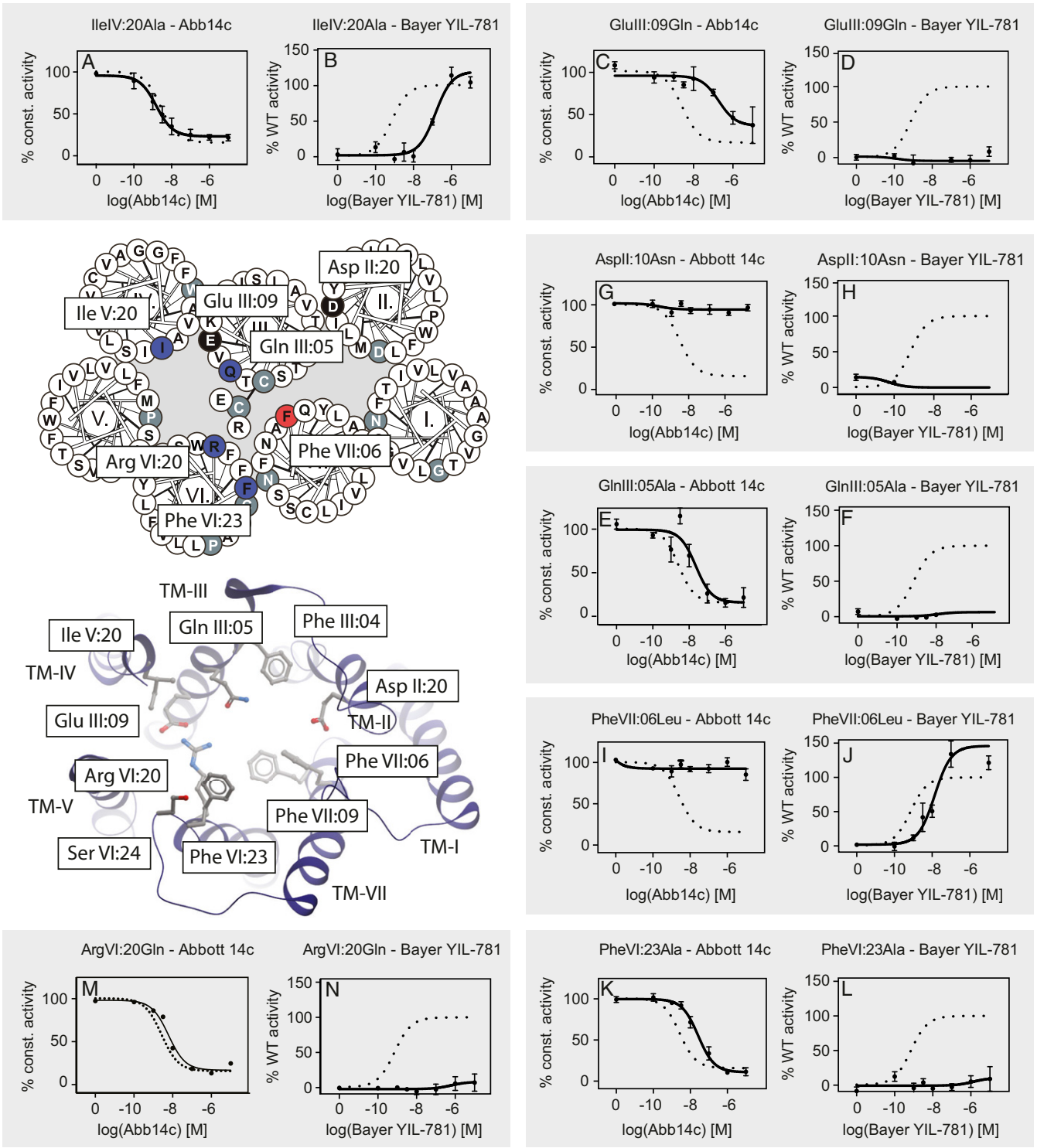

Fig. 4. Substitutions in the GhrR that affect the potency of Abb14c and YIL781. In the helical wheel of the GhrR, residues are indicated with the following color code: red, selective potency shift for Abbott 14c; blue, selective potency shift for Bayer YIL781; black, potency shift for both Abbott 14 and Bayer YIL781. Residues that are substituted and tested but do not affect the signaling properties are indicated in gray. Below the helical wheel is shown a molecular model of the ghrelin receptor based on the X-ray crystal structure of the neurotensin receptor 1 (PDB 4GRV) shown from the extracellular side, where the seven helical domains are presented as cartoon with selected residues shown in stick representation. ECL2 was omitted for clarity. The image was made with ICM, Molsoft L.L.C. Dose–response curves are shown for selected GhrR mutants (solid lines) compared with the wild-type GhrR (dotted lines). Data points are given as the mean ± SEM of three to nine independent experiments performed in triplicate.

Transmembrane domains TMII, TMIII, and TMIV. AspII:10 is a key residue at the top of transmembrane domain TMII, which has previously been recognized as a major interaction point for both inverse agonists and agonists on the GhrR (29). Similarly, the activity of both YIL781 and Abb14c was completely abolished when AspII:10 was replaced by Asn (Fig. 4 and *SI Appendix*, Table S3). GlnIII:05Ala and GluIII:09Gln substitutions also completely abolished the activity of the partial agonist YIL781 but only decreased the potency of the inverse agonist Abb14c (Fig. 4 and *SI Appendix*, Table S3). A similar trend was observed with the IleIV:20Ala substitution, which decreased the potency of the partial agonist more than 100-fold but had no effect on the potency of the inverse agonist (Fig. 4).

Transmembrane domains TMVI and TMVII. PheVI:23 at the top of transmembrane domain TMVI is an important agonist interaction site (29), and Ala-substitution of this residue was also detrimental for the activation by the partial agonist YIL781. In contrast, the mutation decreased the potency of Abb14c by only ∼10-fold. Likewise, substitution of ArgVI:20, which is one of the residues that maintain GhrR in the constitutively active conformation, eliminated the activation by YIL781, whereas the potency of Abb14c was unaffected.

Substitution of PheVII:06 by Leu completely abolished the inverse agonism of Abb14c, whereas YIL781 showed only an eightfold decrease in potency.

In summary, the inverse agonist activity was dependent on only a few residues in the upper part of the transmembrane segment located between transmembrane domains TMII and VII (red and black residues in Fig. 4). In contrast, the biased partial agonist YIL781 was dependent on several interaction points covering a much broader part of the transmembrane region including transmembrane domains TMIII, TMIV, TMVI, and TMVII and also reaching TMII (blue and black residues in Fig. 4).

Based on the functional differences in signaling properties, with Abb13d and Abb14c being inverse agonists and YIL781 being a biased agonist with partial agonist properties in $G\alpha_{q/11}$ and $G\alpha_{12}$ coupling, we used these compounds to translate the signaling properties to in vivo physiological function. Abb13d is chemically very similar to the highly potent Abb14c, but it has more useful pharmacokinetic properties for in vivo studies, e.g., better blood brain penetrance (22). Thus, Abb13d was used for the in vivo studies.

In Vivo Profile of the Small-Molecule Ligands. Both Abb13d and YIL781 have previously been reported to decrease food intake and body weight in rodent models (21, 22). Given their distinct efficacy profiles, we reevaluated the effect of Abb13d and YIL781 on food intake and additionally monitored the effect of the ligands on gastric emptying. Food intake is regulated by a complex interplay between various brain regions and the gut (32). Inhibition of gastric emptying may translate into nausea, thus leading to reduced food intake (33), whereas hypothalamic suppression of food intake is a more direct measure of the homeostatic appetite (34, 35).

Food intake. To investigate the hypothalamic effects of the two compounds exclusively without influences from gastric emptying, we used intracerebroventricular (ICV) administration into the lateral ventricle of the rat brain. The administrations were performed while the rats were housed in specialized cages for continuous monitoring of feeding behavior (30). Both YIL781 and Abb13d were initially administered just before the beginning of the dark phase, when the appetite and plasma ghrelin levels are high. These conditions were regarded as optimal for monitoring potential inhibitory effects on food intake. Surprisingly, only Abb13d decreased food intake, which was observed after 1 h and continued for ∼5 h after administration, whereas YIL781 had no significant effect on food intake at either time point (Fig. 5*A*). In contrast, when the partial agonist YIL781 was administered during the early light phase, when the rats are generally asleep and when plasma ghrelin levels are too low to induce food intake, a significant increase in food intake was observed during the first 30 min after administration. No effect was observed for Abb13d under these conditions (Fig. 5*B*). This is consistent with the fact that YIL781 is a partial agonist for the $G\alpha_{q/11}$ and $G\alpha_{12}$ pathways and that the low circulating level of plasma ghrelin may unmask the agonistic properties of YIL781.

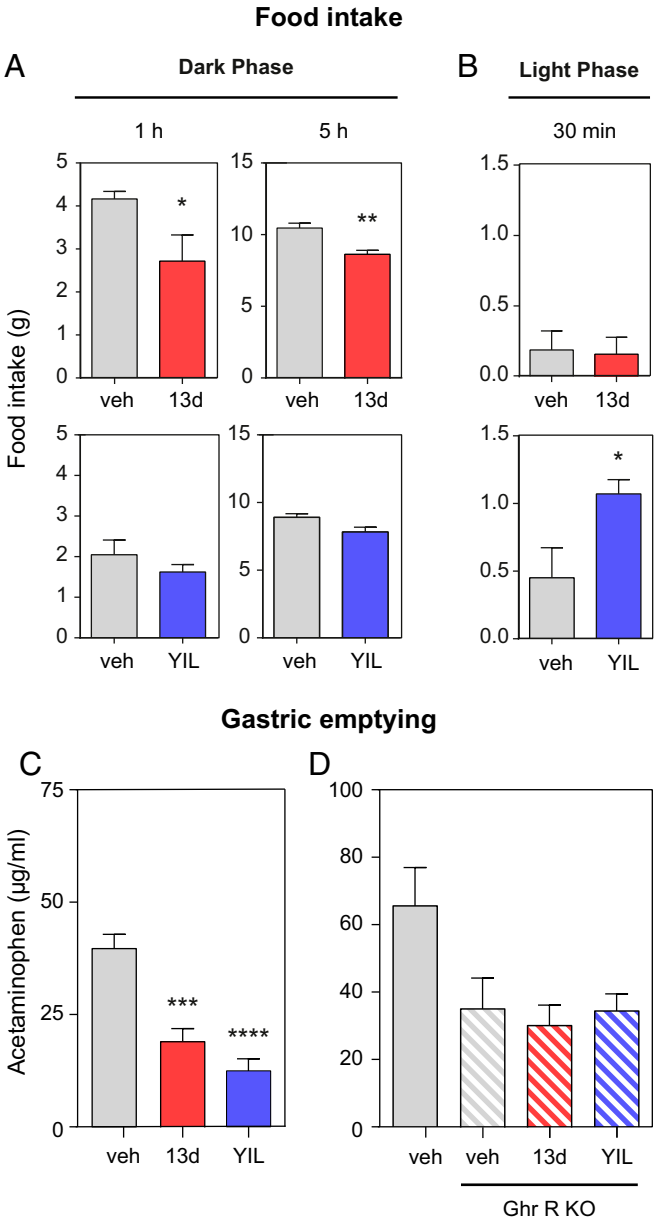

Fig. 5. Effects of YIL781 and Abb13d on food intake and gastric emptying. (*A* and *B*) Food intake in rats after IVC administration of YIL781 and Abb13d just before onset of dark phase (*A*) and during the light phase (*B*) (vehicle, $n = 7$; compound, $n = 8$). (*C* and *D*) Gastric emptying, measured as plasma acetaminophen, in mice after oral administration of YIL781 and Abb13d in wild-type mice ($n = 8$) (*C*) and GhrR-deficient mice ($n = 8$) (*D*). $^{*}P < 0.05$, $^{**}P < 0.01$, $^{***}P < 0.001$, $^{****}P < 0.0001$ based on unpaired Student's *t* test (*A* and *B*) or one-way ANOVA (*C* and *D*). Data represent mean ± SEM. 13d, Abb13d; veh, vehicle; YIL, YIL781.

Gastric emptying. In this assay, YIL781 and Abb13d were administered orally 1 h before acetaminophen administration, which was afterward measured in plasma as an indication of gastric emptying. The study was performed 4 h after onset of the light phase, when plasma ghrelin is low. Gastric emptying was strongly decreased by both Abb13d and YIL781 (Fig. 5*C*). However, the effect of the compounds was completely abolished in GhrR-KO mice (Fig. 5*D*), showing that the effect is indeed mediated through the GhrR. In accordance with previous results, vehicle-treated wild-type mice showed faster gastric emptying than GhrR-deficient mice (Fig. 5*D*) (1), confirming the role of constitutive activity of the GhrR in gastric emptying. This suggests that the partial agonism of YIL781 in the $G\alpha_{q/11}$ and $G\alpha_{12}$ pathways was not sufficient to increase gastric emptying and may indicate that a different signaling pathway including other G proteins or β-arrestin recruitment is involved in this in vivo function.

Knockout of $G\alpha_{q/11}$ in AgRP Neurons. Publically available transcriptomics data for AgRP neurons (36) show high gene-expression levels of $G\alpha_q$ and $G\alpha_{11}$, low expression of $G\alpha_{14}$, and undetectable levels of $G\alpha_{15}$ (*SI Appendix*, Fig. S2*A*). $G\alpha_{12}$, $G\alpha_{13}$, and β-arrestins 1 and 2 are also expressed in AgRP neurons (*SI Appendix*, Fig. S2 *B* and *C*).

To verify the importance of the $G\alpha_{q/11}$ pathway for the ghrelin-mediated increase in food intake, we developed a mouse strain in which $G\alpha_{11}$ was globally deleted and $G\alpha_q$ was removed selectively in AgRP neurons (Fig. 6*A*). This mouse strain was generated by cross-breeding AgRP-Cre mice with the $Gaq^{fl/fl}$; $Ga11^{-/-}$ strain (37, 38). The mice were viable, and the breeding followed normal Mendelian distribution. They developed normally in terms of body weight, body length, and body composition (*SI Appendix*, Fig. S3*A*).

Under basal conditions, the $G\alpha_{q/11}$-deficient mice did not show any differences with respect to food intake (Fig. 6*B*), spontaneous activity (*SI Appendix*, Fig. S3*B*), or energy expenditure (*SI Appendix*, Fig. S3*C*) compared with the control ($G\alpha_{11}$-KO) mice. The s.c. administration of ghrelin (2 mg/kg) induced an acute increase in food intake after 1 h in both $G\alpha_{q/11}$-deficient mice and control mice. However, the ghrelin-induced food intake was significantly reduced in $G\alpha_{q/11}$-KO mice compared with the control mice. After 2 h, no significant ghrelin-promoted food intake could be detected in the $G\alpha_{q/11}$-deficient mice, in contrast to the sustained response observed in the control littermates. ICV administration of the biased agonist YIL781 also increased the food intake in the control mice. However, this response was blunted in the $G\alpha_{q/11}$-deficient mice (Fig. 6), suggesting that $G\alpha_{q/11}$ signaling in the AgRP neurons is indeed important for appetite regulation. In a similar way, we generated a mouse strain in which $G\alpha_{12}$ was globally deleted and $G\alpha_{13}$ was removed selectively in AgRP neurons to test the role of the $G\alpha_{12/13}$ pathway for ghrelin-induced food intake. We observed no difference in the ghrelin-induced food intake of $G\alpha_{12/13}$-KO mice and control mice (*SI Appendix*, Fig. S4). These data indicate that the sustained ghrelin-induced effect on food intake requires the $G\alpha_{q/11}$ pathway and that $G\alpha_{12/13}$ signaling is not involved.

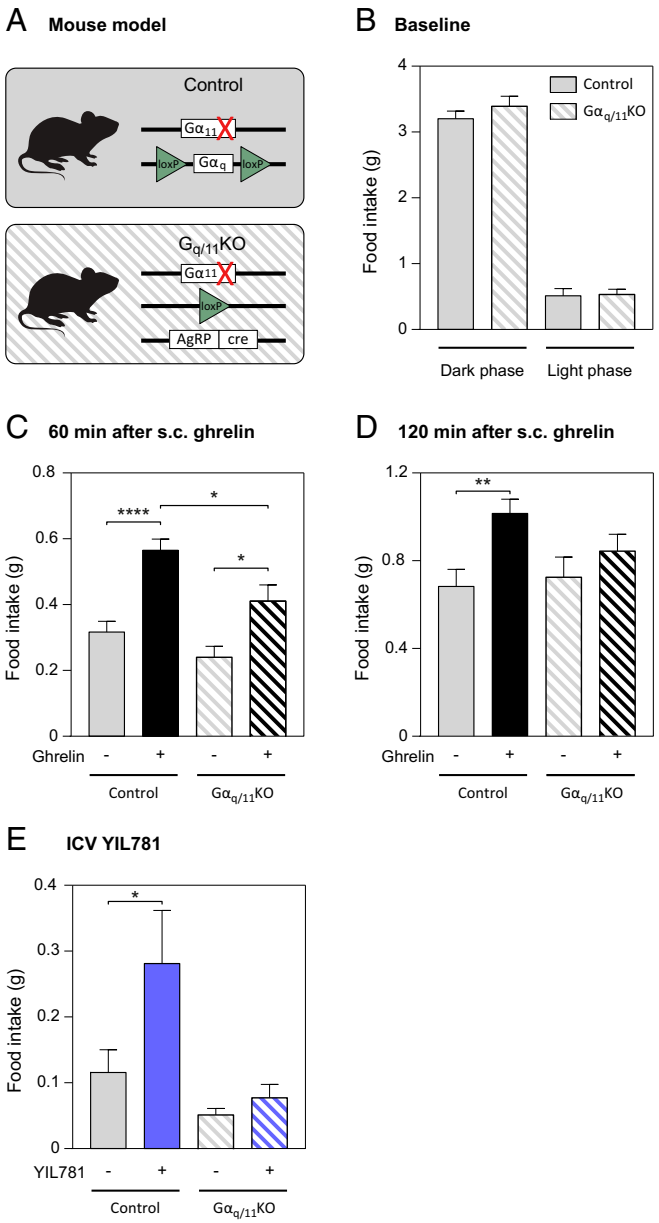

Fig. 6. Food intake in $G\alpha_{q/11}$-KO mice. (*A*) Schematic illustrating the mouse model lacking $G\alpha_{11}$ globally and $G\alpha_q$ specifically in AgRP neurons ($G\alpha_{q/11}$-KO) and the global $G\alpha_{11}$-KO mouse used as control. (*B*) Food intake under basal conditions, averaged over 5 d in $G\alpha_{q/11}$-KO mice ($n = 8$) and controls ($n = 8$). (*C* and *D*) Food intake 1 h (*C*) and 2 h (*D*) after s.c. ghrelin administration (2 mg/kg) in $G\alpha_{q/11}$-KO mice ($n = 12$) and controls ($n = 18$) just before the dark phase. (*E*) Food intake 4 h after ICV administration of YIL781 during the light phase in $G\alpha_{q/11}$-KO mice ($n = 6$) and controls ($n = 7$). $^*P < 0.05$, $^{**}P < 0.01$, $^{****}P < 0.0001$ based on two-way ANOVA followed by Tukey's post hoc test. Data represent mean ± SEM.

Discussion

In this study, we used pharmacological compounds for the GhrR as tools to dissect the physiological importance of different Gα subunits and β-arrestin signaling on food intake and gastric emptying. A biased ligand, YIL781, which selectively activates $G\alpha_{q/11}$ and $G\alpha_{12}$ but has no intrinsic activity for β-arrestin recruitment, was found to increase food intake and decrease gastric emptying. In contrast, Abb13d, which is an inverse agonist for $G\alpha_{q/11}$, decreased both food intake and gastric emptying. This suggests that GhrR-mediated $G\alpha_{q/11}$ activation promotes homeostatic food intake, while other pathways are responsible for GhrR-promoted gastric emptying. The role of $G\alpha_{q/11}$ in GhrR-mediated appetite regulation was confirmed by the reduced YIL781- and ghrelin-induced food intake we observed in mice lacking both $G\alpha_q$ and $G\alpha_{11}$ in AgRP neurons in the hypothalamus, the main neuronal population targeted by ghrelin.

Previous studies reported the ability of the GhrR to engage various signaling pathways (2, 39). Using a combination of second-messenger measurements and various BRET-based sensors, we confirmed that ghrelin activation of its receptor leads to the activation of $G\alpha_{q/11}$, $G\alpha_{i/o}$, and $G\alpha_{12/13}$ family members. Of note, GhrR

PHARMACOLOGY

was found to activate both $G\alpha_{12}$ and $G\alpha_{13}$ in response to ghrelin. This contrasts with a previous study indicating that only $G\alpha_{13}$, but not $G\alpha_{12}$, was activated by the GhrR (39). The difference between the two studies may result from different sensitivities of the biosensors used. The $G\alpha/\beta\gamma$ separation-based sensor utilized in the study by M'Kadmi et al. used $G\gamma$2-GFP10 as the energy acceptor, whereas $G\gamma$1-GFP10 was used for the $G\alpha/\beta\gamma$ separation-based sensor used in the present study. The activation of both $G\alpha_{12}$ and $G\alpha_{13}$ was also confirmed in the present study using the GRK2-based sensor, supporting the notion that these two G proteins can be activated by the GhrR. The GRK2-based BRET biosensors also allowed us to study a broad array of signaling pathways that can be employed by GhrR, allowing us to demonstrate that the entire $G\alpha_{q/11}$ family ($G\alpha_q$, $G\alpha_{11}$, $G\alpha_{14}$, and $G\alpha_{15}$) can be activated by ghrelin with similar efficacy and potency. We also show that the GhrR can activate $G\alpha_z$, the atypical PTX-insensitive member of the $G\alpha_{i/o}$ family.

Our study also shows that compounds developed as antagonists for the GhrR can have distinct intrinsic efficacy profiles. Whereas Abb13d and Abb14c are inverse agonists for the $G\alpha_{q/11}$ pathway, compounds such as Glaxo755053, JMV3002, and YIL781 are partial agonists for this pathway. For the other pathways engaged by ghrelin, the compounds chosen as representative of these two profiles—Abb13d and YIL781—were both neutral antagonists or tended to have very weak inverse efficacy, except in the case of $G\alpha_{12}$ for which YIL781 showed partial agonism. However, this partial agonism was detected only by the most sensitive GRK2-based biosensor. The biased partial agonism toward $G\alpha_{q/11}$ observed for YIL781 is similar to what has previously been described in the characterization of a series of peptide-based GhrR ligands. For these peptides it was shown that partial agonists for $G\alpha_{q/11}$ coupling were neutral antagonists in a β-arrestin 2 recruitment assay (39).

An exciting prospect is the possibility of using biased ligands to develop improved drugs that can target specific functions through selective effects on only a restricted subset of the possible signaling pathways for a given receptor. Mutations in the intracellular loops of GhrR have previously been described to stabilize the receptor in conformational states that selectively activate either $G\alpha_{q/11}$ or β-arrestin and $G\alpha_{i/o}$ (40), indicating that such biased conformations can be achieved. Due to the biased properties of YIL781, which is a partial agonist for $G\alpha_q$, $G\alpha_{11}$, and $G\alpha_{12}$ but a neutral antagonist or weak inverse agonist in the engagement of other signaling pathways, i.e., $G\alpha_{i(1,2,3)}$, $G\alpha_{(oA,oB)}$, $G\alpha_z$, $G\alpha_{13}$, $G\alpha_{14}$, $G\alpha_{15}$, and β-arrestins 1/2, this compound represents a useful tool for uncovering the physiological importance of the different signaling pathways.

The inverse agonist Abb13d decreased both food intake and gastric emptying, whereas the biased agonist YIL781 differentiated between these two physiological functions. It inhibited gastric emptying while having no effect on hypothalamic-mediated food intake in the dark phase, when ghrelin concentration is high, and increasing food consumption in the light phase, when plasma ghrelin levels are low (41) and the basal appetite is accordingly weak. Given the signaling properties of the two ligands, these data clearly indicate a role for $G\alpha_{q/11}$ and possibly $G\alpha_{12}$ activation in the centrally mediated stimulatory effect of ghrelin on appetite and food intake. The observation that the partial agonism of YIL781 can result in an increase in food intake may help explain previous unexpected findings that presumed GhrR antagonists increased food intake and body weight (42, 43). It is possible that these "antagonists" may also act as biased agonists with partial agonistic function on $G\alpha_{q/11}$ or $G\alpha_{12}$ coupling. Testing this hypothesis will require the full signaling characterization of these peptide ligands.

To substantiate the significance of $G\alpha_{q/11}$ for ghrelin-mediated increase in food intake, we selectively deleted $G\alpha_{q/11}$ in AgRP neurons in the arcuate nucleus. In this mouse model, ghrelin increased food intake only temporarily in the first hour after s.c. ghrelin administration, suggesting other signaling pathways contribute slightly to the ghrelin-induced effect on food intake. This may be because $G\alpha_{q/11}$ is removed only in AgRP neurons, and the GhrR is also expressed in other cell types. In addition, it is possible that $G\alpha_{14}$ or $G\alpha_{15}$, which are expressed at low levels under normal conditions, are up-regulated in this knockout model. The fact that YIL781, which is a partial agonist for both $G\alpha_{12}$ and $G\alpha_{q/11}$, increased food intake suggests $G\alpha_{12}$ as an alternative mediator of appetite regulation. However, food intake in mice lacking $G\alpha_{12/13}$ in AgRP neurons was not affected. The approach of selectively knocking out specific G proteins in a hypothalamic neuron population has previously been applied by Lee Weinstein and coworkers to dissect the signaling outcomes of the MC4 receptor regarding appetite regulation versus blood pressure regulation (38). That study showed that $G\alpha_q$ coupling is required for the modulation of food intake, whereas the unwanted effect on blood pressure is dependent on $G\alpha_s$ coupling. Hence, this study precipitated further effort to develop a $G\alpha_{q/11}$-biased ligand. Our knockout of $G\alpha_{q/11}$ in AgRP neurons may precipitate the development of inverse agonists for GhrR targeting the $G\alpha_{q/11}$ pathway. The lack of a metabolic phenotype in mice lacking $G\alpha_{q/11}$ in AgRP neurons may not be surprising and most likely results from compensatory mechanisms during embryonic development. It is commonly observed that knockout models do not reveal a phenotype under basal conditions; however, it is possible that metabolic challenges, such as exposure to a high-fat diet, could uncover a phenotype as observed for the global GhrR knockout (44). In other cases, such as the GLP-1 receptor, which is a validated antiobesity target, a high-fat diet does not reveal any phenotype (45).

When considering gastric emptying, one cannot fully exclude the possibility that the inhibition of gastric emptying results from the complete or partial inhibition of $G\alpha_{q/11}$ promoted by Abb13d and YIL781, respectively, keeping in mind that a partial agonist is also a partial antagonist. However, it would be somewhat surprising if the inverse agonist and the partial agonist had the same effect on gastric emptying, especially given that gastric emptying is under tonic control of the GhrR, as illustrated by the significantly slower gastric emptying observed in the GhrR-KO mice. Therefore it is more likely that the inhibition of gastric emptying by both Abb13d and YIL781 results from the blockade of one or some of the other pathways engaged by GhrR, presumably through neutral antagonism or inverse agonism at the β-arrestin, $G\alpha_{i/o}$, or $G\alpha_{13}$ pathways. To address this issue, it would be interesting in a future study to test how the compounds work in a β-arrestin–KO model. In particular, the effect of the biased compound and ghrelin in mice with β-arrestin deficiency selectively in the enteric neurons would be highly interesting.

Differentiating Abb13d and YIL781 by their action on food intake and gastric emptying, given their different signaling profiles, may have important implications for the development of drugs targeting GhrR-mediated food intake. Indeed, nausea, a side effect often plaguing antiobesity drug development, may be related to a reduction of gastric emptying. For example, the therapeutic effect of the successful antiobesity drug liraglutide, a GLP1 receptor antagonist, is based on its hypothalamically mediated anorexigenic effect. However, nausea is a common adverse effect in many patients, sometimes leading to discontinuation of the treatment (33, 34). It has been suggested that decreased gastric emptying through an effect on the area postrema of the brain and the enteric nervous system is the cause of such nausea (38). Since ghrelin increases gastric emptying and the activity of the enteric nervous system, GhrR antagonists could lead to similar nausea caused by decreased gastric emptying.

Based on our data, we suggest that a compound with inverse agonistic activity on $G\alpha_{q/11}$ but partial agonism on some or all of the other GhrR-engaged pathways is a favorable choice to promote appetite reduction without affecting gastric emptying.

Materials and Methods

Cell Culture and Transfection. HEK293 cells were cultured at 10% CO_2, 90% humidity, and 37 °C in DMEM with GlutaMAX (Gibco) supplemented with 10% FBS, 100 U/mL penicillin, and 0.1 mg/mL streptomycin.

For binding, IP, and Ca^{2+} assays, HEK293 cells were seeded in poly-D-lysine–coated 96-well plates (PerkinElmer) the day before transfection, at a density of 30,000 cells per well. Transient transfections were performed using Lipofectamine 2000 (Thermo Fisher) according to the manufacturer's instructions. Cells were transfected with 20 ng DNA (pCMV-hGhrR or empty pCMV) and 0.6 μL Lipofectamine 2000 per well for 5 h. Binding, IP, and Ca^{2+} assays were performed 48 h after the transfection was started.

For BRET assays, HEK293 cells were seeded in white poly-D-lysine–coated 96-well plates (PerkinElmer) the day before transfection, at a density of 30,000 cells per well. Transient transfections were performed using linear polyethylenimine (PEI) (Polysciences, Inc.), at a PEI:DNA ratio of 3:1, as a transfection reagent. After overnight incubation in the transfection mix, fresh medium was added. BRET assays were performed 48 h after the transfection was started.

Binding. Competition binding experiments were performed for 3 h at 4 °C using 25 pM ^{3}H-labeled MK-677. Binding assays were performed in 100 μL of 50 mM Hepes buffer, pH 7.4, supplemented with 1 mM $CaCl_2$, 5 mM $MgCl_2$, 0.1% (wt/vol) BSA, and 40 μg/mL bacitracin. Nonspecific binding was determined as the binding in the presence of 1 μM unlabeled ghrelin. Cells were washed twice in ice-cold buffer. Fifty microliters of lysis buffer/scintillation fluid (30% ethoxylated alkylphenol and 70% diisopropylnaphthalene isomers) was added, and the bound radioactivity was counted. Determinations were made in triplicate.

Ca^{2+} Mobilization. Two days after transfection, HEK293 cells were incubated in loading buffer (HBSS supplemented with 20 mM Hepes, 1 mM $CaCl_2$, 1 mM $MgCl_2$, 0.7 mg/mL probenicid, 0.2% Fluo-4) (50 μL per well) containing the Ca^{2+}-sensitive fluorophore (Fluo-4 AM, Life Technologies). The cells were incubated for 1 h at 37 °C and then were washed twice in wash buffer (HBSS containing 20 mM Hepes, 1 mM $CaCl_2$, 1 mM $MgCl_2$, 0.7 mg/mL probenicid). Cells were incubated in 100 μL of wash buffer in a FlexStation 3 microplate reader (Molecular Devices) for 5 min. Measurements were performed at 37 °C. A 485-nM excitation filter and 520-nM emission filter were used. Ligands (15 μL) were added at an injection speed of 2 μL/s. To test for antagonism, compounds were added 30 min before ghrelin was injected.

IP-Accumulation Assay. One day after the transfection, HEK293 cells were incubated in cell-culture medium containing 5 μCi/mL myo-[2-^{3}H]inositol. Following 24-h incubation, the cells were washed in HBSS (Gibco) and were incubated in HBSS containing 10 mM LiCl (100 μL per well) for 30 min at 37 °C. The ligands were added, and the cells were incubated for 45 min at 37 °C. To test for antagonism, the cells were preincubated with the compounds for 30 min; then ghrelin was added, and the cells were incubated for 45 min at 37 °C. The cells were then lysed in 10 mM formic acid for >40 min. Twenty microliters of the lysate was transferred to a white 96-well plate containing 80 μL of yttrium silicate Scintillation Proximity Assay (YSi-SPA) beads (PerkinElmer). Lyophilized YSi-SPA beads were reconstituted in H_2O (1 g in 10 mL) and then were diluted 1:8 before use. Plates were sealed, shaken at maximum speed for 10 min, and centrifuged at 400 × *g* for 5 min. After an 8-h delay, γ-radiation was measured in a Packard Top Count NXT scintillation plate reader. Determinations were made in duplicate or triplicate.

BRET Assay. BRET assays were performed as described previously (28, 46, 47). Proteins were fused to RlucII as the energy donor and modified GFPs (GFP10 or rGFP) as the energy acceptor.

To measure the interaction between Gγ5 and GRK2 (using a GRK2-based BRET biosensor detecting G-protein activation), HEK293 cells were cotransfected with human GhrR, GRK2-GFP10, RlucII-$G\gamma_5$, or $G\beta_1$ in the absence (control) or presence of the tested Gα subunit (48, 49). As an alternative to the GRK2-based BRET biosensor, activation of G proteins was confirmed by monitoring the separation between Gα and $G\gamma_1$ in HEK293 cells. Gβ1 was cotransfected with human GhrR, Gα subunits tagged with RlucII, and Gγ1 tagged with GFP10 at the N terminus (28). To measure the recruitment of β-arrestins by GhrR, we assessed its translocation to the plasma membrane using an enhanced bystander BRET-based biosensor (50) that monitors BRET between RlucII attached to β-arrestin-1 or β-arrestin-2 and rGFP anchored to the plasma membrane. For this purpose, HEK293 cells were cotransfected with human GhrR, β-arrestin1/2-RlucII and rGFP-CAAX (CAAX being the membrane-anchoring protein motif of KRas) (50).

Forty-eight hours after transfection, cells were washed in HBSS and incubated in 90 μL of Tyrode's buffer for 2 h at 37 °C. Then, cells were incubated with 10 μL of ligand for 10 min. The luciferase substrate coelenterazine 400a at a concentration of 2.5 μM was added 5 min before BRET reading. BRET was measured using a Synergy Neo microplate reader (BioTek) equipped with an acceptor filter (515 ± 30 nm) and donor filter (410 ± 80 nm). The BRET signal was determined as the ratio of light emitted by the acceptor (GFP10 or rGFP) to that emitted by the donor (RlucII). The agonist-promoted BRET signal (ΔBRET) is the difference in BRET recorded from cells treated with agonist and cells treated with vehicle. For the GRK2-based biosensor, the results are expressed as a BRET ratio, i.e., the ratio of BRET obtained with ligand treatment to BRET obtained with vehicle treatment. The results are then presented as the BRET ratio obtained from cells transfected with the tested Gα subunit to the BRET ratio obtained from the control transfection (without cotransfection of a Gα subunit), to correct for the activation induced by endogenous Gα subunits.

Genetic Mouse Models. To study the role of ghrelin-mediated $G\alpha_{q/11}$-signaling in AgRP neurons, we generated mice lacking both $G\alpha_{11}$ globally and $G\alpha_q$ in AgRP neurons ($Gnaq^{fl/fl}$; $Gna11^{-/-}$; AgRP-$cre^{+/-}$ mice, herein referred to as "$G\alpha_{q/11}$-KO" mice). $Gnaq^{fl/fl}$; $Gna11^{-/-}$ mice are similar to wild-type littermates and have a normal metabolic phenotype (37, 38) and were thus used as controls (*SI Appendix*, Fig. S3). In parallel, we generated mice lacking both $G\alpha_{12}$ globally and $G\alpha_{13}$ in AgRP neurons ($Gna13^{fl/fl}$; $Gna12^{-/-}$; AgRP-$cre^{+/-}$ mice, herein referred to as "$G\alpha_{12/13}$-KO" mice) to investigate if GhrR–$G\alpha_{12/13}$ coupling contributed to the orexigenic effect of ghrelin.

Animals were maintained on a 12-h light/dark cycle and had ad libitum access to water and a chow diet (Altromin no. 1314; Brogaarden) unless otherwise stated. The studies in mice and rats were approved by the Danish Animals Inspectorate and were performed according to institutional guidelines.

The experiments were done in a 16-chamber indirect calorimetry system (PhenoMaster; TSE Systems). Before any experiment, the animals were allowed at least 5 d for adaptation to the new cages and single housing. Three conditions were measured: baseline measurements, response to fasting, and response to a single s.c. ghrelin administration. For the fasting study, the mice were fasted for 24 h, starting in the beginning of the dark phase. The mice had free access to water. The s.c. ghrelin administrations (2 mg/kg; Polypeptide) were likewise done immediately before the dark phase.

Before the beginning of the study, fat and lean mass of unanesthetized mice was assessed by quantitative MRI using EchoMRI (Echo Medical Systems).

ICV Administrations of Abb13D and YIL781. Male Sprague–Dawley rats (Taconic) were anesthetized with 0.27 mL/kg Hypnorm/midazolam (fentanyl citrate, 0.07875 mg/mL; fluanisone, 2.5 mg/mL; and midazolam, 1.25 mg/mL). After 30 min, 5 mg/kg Rimadyl (Pfizer) was given s.c., and the rat was fixed in a stereotaxic instrument. The skull was exposed with a sagittal incision on the midline of the scalp, a hole was drilled, and a stainless steel guide cannula was positioned 1.0 mm posterior to bregma and 1.5 mm lateral to the midline. To secure the cannula, two 1.0-mm stainless steel anchor screws (AgnThos) were attached to the skull, and dental cement (Poly-F Plus; Dentsply) was applied. Postoperatively the rats received 5 mg/kg Rimadyl once a day for 3 d. The rats were allowed at least 1 wk for recovery after the surgery. To test the placement of the cannula, the drinking response to human Angiotensin II (Sigma-Aldrich) was monitored; only rats that drank more than 6 mL within the first half hour were included in the study. Compounds were administered during the light phase or immediately before the dark phase. Immediately after the injection, the rat was returned to its home cage, and food intake was recorded using MANI FeedWin cases (Ellegaard Systems).

Gastric Emptying. Rates of gastric emptying were determined using plasma concentrations of acetaminophen after oral administration. Mice were fasted overnight and given 100 mg/kg acetaminophen in sterile water. Blood samples were drawn in heparinized blood-collection tubes just before and 15 and 60 min or 20 and 40 min after acetaminophen administration. Ligands were administered orally 1 h before oral administration of acetaminophen, which was afterward quantified in plasma as a measurement of gastric emptying. Plasma acetaminophen concentrations were measured using an acetaminophen assay kit (Abbott).

Calculations and Data Analysis. Data were plotted and tested for statistical significance using GraphPad Prism version 7.02 for Windows (GraphPad Software).

EC_{50} values of dose–response curves were determined by nonlinear regression.

The statistical significance for comparisons of food intake in the $G_{q/11}$-KO and control mice was determined by a two-way ANOVA with Tukey's multiple-comparisons test. For the continued analysis of food intake over

time, a two-way repeated-measures ANOVA and Sidak's multiple comparisons test were used. Comparison of food intake in rats was determined by Student's *t* tests.

Statistical significance for comparisons of gastric emptying in wild-type and GhrR-KO mice was determined by a one-way ANOVA with Dunnett's multiple-comparisons test for both sets of data. Statistical significance is denoted as $*P < 0.05$, $**P < 0.01$, $***P < 0.001$, $****P < 0.0001$.

ACKNOWLEDGMENTS. We thank Christian LeGouill and Viktoryia Lukasheva, who developed the GRK2-based BRET biosensor used in this study, and Siv A. Hjort for careful proofreading of the manuscript. This study was supported by a grant from the Novo Nordisk Foundation Center for Basic Metabolic Research and by Canadian Institute for Health Research Foundation Grant FDN148431. The Novo Nordisk Foundation Center for Basic Metabolic Research is supported by an unconditional grant from the Novo Nordisk Foundation to the University of Copenhagen. F.M., C.H., and L.J.S. received PhD scholarships from the Faculty of Health and Medical Sciences, University of Copenhagen. B.P. holds a postdoctoral fellowship from Diabetes Canada, and M.B. holds the Canada Research Chair in Signal Transduction and Molecular Pharmacology.

1. Müller TD, et al. (2015) Ghrelin. *Mol Metab* 4:437–460.
2. Sivertsen B, Holliday N, Madsen AN, Holst B (2013) Functionally biased signalling properties of 7TM receptors–opportunities for drug development for the ghrelin receptor. *Br J Pharmacol* 170:1349–1362.
3. Urban JD, et al. (2007) Functional selectivity and classical concepts of quantitative pharmacology. *J Pharmacol Exp Ther* 320:1–13.
4. Whalen EJ, Rajagopal S, Lefkowitz RJ (2011) Therapeutic potential of β-arrestin- and G protein-biased agonists. *Trends Mol Med* 17:126–139.
5. Howard AD, et al. (1996) A receptor in pituitary and hypothalamus that functions in growth hormone release. *Science* 273:974–977.
6. Bennett KA, Langmead CJ, Wise A, Milligan G (2009) Growth hormone secretagogues and growth hormone releasing peptides act as orthosteric super-agonists but not allosteric regulators for activation of the G protein Galpha(o1) by the ghrelin receptor. *Mol Pharmacol* 76:802–811.
7. Damian M, et al. (2012) High constitutive activity is an intrinsic feature of ghrelin receptor protein: A study with a functional monomeric GHS-R1a receptor reconstituted in lipid discs. *J Biol Chem* 287:3630–3641.
8. Mokrosiński J, Frimurer TM, Sivertsen B, Schwartz TW, Holst B (2012) Modulation of constitutive activity and signaling bias of the ghrelin receptor by conformational constraint in the second extracellular loop. *J Biol Chem* 287:33488–33502.
9. Reiter E, Ahn S, Shukla AK, Lefkowitz RJ (2012) Molecular mechanism of β-arrestin-biased agonism at seven-transmembrane receptors. *Annu Rev Pharmacol Toxicol* 52: 179–197.
10. Kenakin T (2015) The effective application of biased signaling to new drug discovery. *Mol Pharmacol* 88:1055–1061.
11. Galandrin S, Oligny-Longpré G, Bouvier M (2007) The evasive nature of drug efficacy: Implications for drug discovery. *Trends Pharmacol Sci* 28:423–430.
12. Noma T, et al. (2007) β-arrestin-mediated β1-adrenergic receptor transactivation of the EGFR confers cardioprotection. *J Clin Invest* 117:2445–2458.
13. Appleton KM, et al. (2013) Biasing the parathyroid hormone receptor: Relating in vitro ligand efficacy to in vivo biological activity. *Methods Enzymol* 522:229–262.
14. Gesty-Palmer D, et al. (2009) A beta-arrestin-biased agonist of the parathyroid hormone receptor (PTH1R) promotes bone formation independent of G protein activation. *Sci Transl Med* 1:1ra1.
15. Urs NM, et al. (2016) Distinct cortical and striatal actions of a β-arrestin-biased dopamine D2 receptor ligand reveal unique antipsychotic-like properties. *Proc Natl Acad Sci USA* 113:E8178–E8186.
16. Urs NM, Peterson SM, Caron MG (2017) New concepts in dopamine D_2 receptor biased signaling and implications for schizophrenia therapy. *Biol Psychiatry* 81:78–85.
17. Violin JD, et al. (2010) Selectively engaging β-arrestins at the angiotensin II type 1 receptor reduces blood pressure and increases cardiac performance. *J Pharmacol Exp Ther* 335:572–579.
18. Manglik A, et al. (2016) Structure-based discovery of opioid analgesics with reduced side effects. *Nature* 537:185–190.
19. DeWire SM, et al. (2013) A G protein-biased ligand at the μ-opioid receptor is potently analgesic with reduced gastrointestinal and respiratory dysfunction compared with morphine. *J Pharmacol Exp Ther* 344:708–717.
20. Singla N, et al. (2017) A randomized, Phase IIb study investigating oliceridine (TRV130), a novel μ-receptor G-protein pathway selective (μ-GPS) modulator, for the management of moderate to severe acute pain following abdominoplasty. *J Pain Res* 10:2413–2424.
21. Esler WP, et al. (2007) Small-molecule ghrelin receptor antagonists improve glucose tolerance, suppress appetite, and promote weight loss. *Endocrinology* 148:5175–5185.
22. Xin Z, et al. (2006) Discovery and pharmacological evaluation of growth hormone secretagogue receptor antagonists. *J Med Chem* 49:4459–4469.
23. Holst B, Cygankiewicz A, Jensen TH, Ankersen M, Schwartz TW (2003) High constitutive signaling of the ghrelin receptor–Identification of a potent inverse agonist. *Mol Endocrinol* 17:2201–2210.
24. Kenakin T, Onaran O, Kenakin T (2002) The ligand paradox between affinity and efficacy: Can you be there and not make a difference? *Trends Pharmacol Sci* 23: 275–280.
25. Mokrosiński J, Holst B (2010) Modulation of the constitutive activity of the ghrelin receptor by use of pharmacological tools and mutagenesis. *Methods Enzymol* 484: 53–73.
26. Bonacci TM, et al. (2006) Differential targeting of Gβγ-subunit signaling with small molecules. *Science* 312:443–447.
27. Schrage R, et al. (2015) The experimental power of FR900359 to study Gq-regulated biological processes. *Nat Commun* 6:10156.
28. Galés C, et al. (2006) Probing the activation-promoted structural rearrangements in preassembled receptor-G protein complexes. *Nat Struct Mol Biol* 13:778–786.
29. Holst B, et al. (2009) Overlapping binding site for the endogenous agonist, small-molecule agonists, and ago-allosteric modulators on the ghrelin receptor. *Mol Pharmacol* 75:44–59.
30. Sivertsen B, et al. (2011) Unique interaction pattern for a functionally biased ghrelin receptor agonist. *J Biol Chem* 286:20845–20860.
31. Holst B, et al. (2006) Ghrelin receptor inverse agonists: Identification of an active peptide core and its interaction epitopes on the receptor. *Mol Pharmacol* 70:936–946.
32. Timper K, Brüning JC (2017) Hypothalamic circuits regulating appetite and energy homeostasis: Pathways to obesity. *Dis Model Mech* 10:679–689.
33. Jelsing J, et al. (2012) Liraglutide: Short-lived effect on gastric emptying—Long lasting effects on body weight. *Diabetes Obes Metab* 14:531–538.
34. Secher A, et al. (2014) The arcuate nucleus mediates GLP-1 receptor agonist liraglutide-dependent weight loss. *J Clin Invest* 124:4473–4488.
35. Sisley S, et al. (2014) Neuronal GLP1R mediates liraglutide's anorectic but not glucose-lowering effect. *J Clin Invest* 124:2456–2463.
36. Henry FE, Sugino K, Tozer A, Branco T, Sternson SM (2015) Cell type-specific transcriptomics of hypothalamic energy-sensing neuron responses to weight-loss. *eLife* 4: 1–30.
37. Offermanns S, et al. (1998) Embryonic cardiomyocyte hypoplasia and craniofacial defects in G α q/G α 11-mutant mice. *EMBO J* 17:4304–4312.
38. Li Y, et al. (2016) Gq/11α and Gsα mediate distinct physiological responses to central melanocortins. *J Clin Invest* 126:1–10.
39. M'Kadmi C, et al. (2015) Agonism, antagonism, and inverse agonism bias at the ghrelin receptor signaling. *J Biol Chem* 290:27021–27039.
40. Evron T, et al. (2014) G protein and β-arrestin signaling bias at the ghrelin receptor. *J Biol Chem* 289:33442–33455.
41. Laermans J, Vancleef L, Tack J, Depoortere I (2015) Role of the clock gene Bmal1 and the gastric ghrelin-secreting cell in the circadian regulation of the ghrelin-GOAT system. *Sci Rep* 5:16748.
42. Costantini VJA, et al. (2011) GSK1614343, a novel ghrelin receptor antagonist, produces an unexpected increase of food intake and body weight in rodents and dogs. *Neuroendocrinology* 94:158–168, and correction (2012) 95:247.
43. Halem HA, et al. (2005) A novel growth hormone secretagogue-1a receptor antagonist that blocks ghrelin-induced growth hormone secretion but induces increased body weight gain. *Neuroendocrinology* 81:339–349.
44. Zigman JM, et al. (2005) Mice lacking ghrelin receptors resist the development of diet-induced obesity. *J Clin Invest* 115:3564–3572.
45. Scrocchi LA, et al. (1996) Glucose intolerance but normal satiety in mice with a null mutation in the glucagon-like peptide 1 receptor gene. *Nat Med* 2:1254–1258.
46. Quoyer J, et al. (2013) Pepducin targeting the C-X-C chemokine receptor type 4 acts as a biased agonist favoring activation of the inhibitory G protein. *Proc Natl Acad Sci USA* 110:E5088–E5097.
47. Paradis JS, et al. (2015) Receptor sequestration in response to β-arrestin-2 phosphorylation by ERK1/2 governs steady-state levels of GPCR cell-surface expression. *Proc Natl Acad Sci USA* 112:E5160–E5168.
48. Karamitri A, et al. (2018) Type 2 diabetes–associated variants of the MT_2 melatonin receptor affect distinct modes of signaling. *Sci Signal* 11:eaan6622.
49. Fuchs T, et al. (2013) Mutations in GNAL cause primary torsion dystonia. *Nat Genet* 45: 88–92.
50. Namkung Y, et al. (2016) Monitoring G protein-coupled receptor and β-arrestin trafficking in live cells using enhanced bystander BRET. *Nat Commun* 7:12178.